



ChemComm

**Scope and mechanism of nitrile dihydroboration mediated  
by a  $\beta$ -diketiminato manganese hydride catalyst**

Journal:	<i>ChemComm</i>
Manuscript ID	CC-COM-12-2019-009921.R2
Article Type:	Communication

SCHOLARONE™  
Manuscripts

## COMMUNICATION

## Scope and mechanism of nitrile dihydroboration mediated by a $\beta$ -diketiminate manganese hydride catalyst

Received 00th January 20xx,  
Accepted 00th January 20xx

Thao T. Nguyen,<sup>a</sup> Jun-Hyeong Kim,<sup>b,c</sup> Suyeon Kim,<sup>b,c</sup> Changjin Oh,<sup>b,c</sup> Marco Flores,<sup>a</sup> Thomas L. Groy,<sup>a</sup> Mu-Hyun Baik<sup>\*b,c</sup> and Ryan J. Trovitch<sup>\*a</sup>

DOI: 10.1039/x0xx00000x

**The manganese hydride dimer,  $[(2,6\text{-}i\text{Pr}_2\text{PhBDI})\text{Mn}(\mu\text{-H})_2]$ , was found to mediate nitrile dihydroboration, rendering it the first manganese catalyst for this transformation. Stoichiometric experiments revealed that benzonitrile insertion affords  $[(2,6\text{-}i\text{Pr}_2\text{PhBDI})\text{Mn}(\mu\text{-NCHC}_6\text{H}_5)]_2$  en route to *N,N*-diborylamine formation. Density functional theory calculations reveal the precise mechanism and demonstrate that catalysis is promoted by monomeric species.**

Borylamines have emerged as promising reagents for organic synthesis. In 2004, Murakami and Suginoe found aminoboranes to be effective iminium ion generators for a 3-component Mannich protocol involving the coupling of aldehydes, secondary amines, and silyl ketene acetals.<sup>1</sup> Nikonov showed that  $\text{PhCH}_2\text{N}(\text{BCat})_2$  reacts with benzaldehyde to yield the corresponding imine without the use of a dehydrating agent (imines are commonly prepared from amines and carbonyls via condensation).<sup>2</sup> In 2019, Tobita was able to prepare *N*-arylimines and *N,N*-diarylamines from the corresponding borylimines and diborylamines using bromoarenes,  $\text{KO}^t\text{Bu}$ ,  $\text{Pd}(\text{dba})_2$ , and  $\text{CyJohnPhos}$ .<sup>3</sup> Moreover, the Jassar and Bertrand groups reported the catalyst-free preparation of primary aminoboranes that chemoselectively react with aldehydes to afford aldimines.<sup>4</sup> Recently, we disclosed the first examples of *N*-substituted amide synthesis using *N,N*-diborylamines and carboxylic acids.<sup>5</sup>

Nitrile dihydroboration is an efficient and mild method to prepare *N,N*-diborylamines. Nikonov initially found that  $(2,6\text{-}i\text{Pr}_2\text{PhN})\text{Mo}(\text{H})(\text{Cl})(\text{PMe}_3)_3$  and  $(2,6\text{-}i\text{Pr}_2\text{PhN})\text{MoH}_2(\text{PMe}_3)_3$  mediate the dihydroboration of benzonitrile and acetonitrile with turnover frequencies (TOFs) of up to  $1.7\text{ h}^{-1}$ .<sup>2,6</sup> In 2015, Szymczak reported the dihydroboration of nitriles using a proton-switchable, bifunctional Ru complex with TOFs of up to  $60\text{ h}^{-1}$ .<sup>7</sup> Gunanathan also found that

$[\text{Ru}(p\text{-cymene})\text{Cl}_2]_2$  can mediate the hydroboration of nitriles and imines with maximum TOFs of  $6.7\text{ h}^{-1}$ .<sup>8</sup> Hill and Ma developed Mg catalysts featuring  $\beta$ -diketiminate ligands for this transformation and reported TOFs of up to  $20\text{ h}^{-1}$ ,<sup>9,10</sup> while Shimada demonstrated nitrile dihydroboration using Ni(II) salts featuring bis(acetylacetonato) ligands in the presence of HBCat under ambient temperature (TOF =  $11\text{ h}^{-1}$ ).<sup>11</sup> Nakazawa achieved nitrile dihydroboration using a binuclear iron-indium complex,  $[\text{Fe}(\text{CH}_3\text{CN})_6][\text{cis-Fe}(\text{CO})_4(\text{InCl}_3)_2]$  (TOF =  $0.4\text{ h}^{-1}$ )<sup>12</sup> and Fout described a Co-pincer catalyst for nitrile dihydroboration at  $70\text{ }^\circ\text{C}$ .<sup>13</sup> In Tobita's recent demonstration of borylamine cross-coupling, it was found that Ru catalysts featuring a bis(silyl)xanthene ligand showed modest activity.<sup>3</sup> Over the last year, nitrile dihydroboration catalysis has been extended to a number of metals including Er,<sup>14</sup> Y,<sup>14</sup> Dy,<sup>14</sup> Gd,<sup>14</sup> Al,<sup>15-17</sup> Th,<sup>18</sup> Ti,<sup>19</sup> and Zn,<sup>20</sup> and has even been catalysed by a Co-H functionalised MOF.<sup>21</sup>

Our group has also contributed to the development of nitrile dihydroboration catalysis. In 2017, we demonstrated that 1.0 mol% of the  $\alpha$ -diimine cobalt hydride complex,  $(\text{Ph}^2\text{PPrDI})\text{CoH}$ , catalyses this transformation at  $60\text{ }^\circ\text{C}$ .<sup>22</sup> Our work to develop a second generation variant that exhibits nitrile dihydroboration TOFs of up to  $380\text{ h}^{-1}$  at  $25\text{ }^\circ\text{C}$ ,  $(\text{PyEt})\text{P}^{\text{CHMe}}\text{N}^{\text{ETPy}}\text{Co}$ , was reported earlier this year.<sup>5</sup> The high activity of this catalyst was attributed to its redox non-innocent ligand, the accessibility of a triplet spin manifold, and the ability of the chelate to promote inner-sphere boryl group transfer. Given recent interest in Mn-based hydrofunctionalisation catalysis,<sup>23-26</sup> we aimed to leverage our study of the  $\beta$ -diketiminate Mn alkene hydrosilylation catalyst,  $[(2,6\text{-}i\text{Pr}_2\text{PhBDI})\text{Mn}(\mu\text{-H})_2]$  (**1**, Figure 1),<sup>27</sup> to demonstrate Mn-catalysed nitrile dihydroboration for the first time.

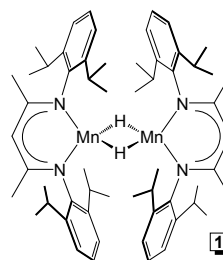


**Figure 1.** Structure of  $[(2,6\text{-}i\text{Pr}_2\text{PhBDI})\text{Mn}(\mu\text{-H})_2]$  (**1**).

<sup>a</sup> School of Molecular Sciences, Arizona State University, Tempe, Arizona, 85287, USA. E-mail: ryan.trovitch@asu.edu; Tel: +1 480 727 8930.

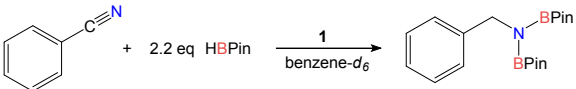
<sup>b</sup> Department of Chemistry, Korea Advanced Institute of Science and Technology (KAIST), Daejeon 34141, Republic of Korea. E-mail: mbaik2805@kaist.ac.kr.

<sup>c</sup> Center for Catalytic Hydrocarbon Functionalizations, Institute for Basic Science (IBS), Daejeon 34141, Republic of Korea.

† Electronic Supplementary Information (ESI) available: Experimental procedures, X-ray crystallographic data for **2** (CCDC – 1973606), product characterization, and computational details. See DOI: 10.1039/x0xx00000x

**Nitrile Dihydroboration.** To begin this study, **1** was prepared and purified following an early procedure.<sup>27</sup> The activity of **1** for benzonitrile dihydroboration was evaluated by monitoring reactions in benzene-*d*<sub>6</sub> by <sup>1</sup>H NMR spectroscopy (Table 1). Pinacolborane (HBPin) was chosen as the borane source and a slight excess was used to promote complete nitrile reduction. In particular, adding 2.2 equiv. of HBPin to benzonitrile in the presence of 2.5 mol% of **1** (5 mol% of Mn) in benzene-*d*<sub>6</sub> resulted in modest conversion after 2 days (27%) at room temperature (entry 1). Heating the same mixture to 60 °C afforded 80% conversion after 2 days (entry 2) and complete conversion was achieved at 80 °C after 12 h (entry 3). Nitrile reduction using other reagents was also evaluated (entry 4-6). Particularly, no reaction was observed between benzonitrile and 9-BBN or phenyl silane under identical conditions, while HBCat gave poor conversion after 24 h. Therefore, HBPin was chosen for **1**-catalysed nitrile dihydroboration. To optimise the conditions, the catalyst loading was lowered to 0.5 mol% (1 mol% Mn), allowing for complete benzonitrile dihydroboration after 24 h at 80 °C (entry 7).

**Table 1.** Optimisation of **1**-catalysed benzonitrile dihydroboration conditions.



Entry	Mol % <b>1</b>	Reductant	Temp. (°C)	Time (h)	% Conv. <sup>a</sup>
1	2.5	HBPin	25	48	27%
2	2.5	HBPin	60	48	80%
3	2.5	HBPin	80	12	99%
4	2.5	9-BBN	80	24	n. r.
5	2.5	PhSiH <sub>3</sub>	80	24	n. r.
6	2.5	HBCat	80	24	9%
7	0.5	HBPin	80	24	99%
8	0	HBPin	80	24	5%

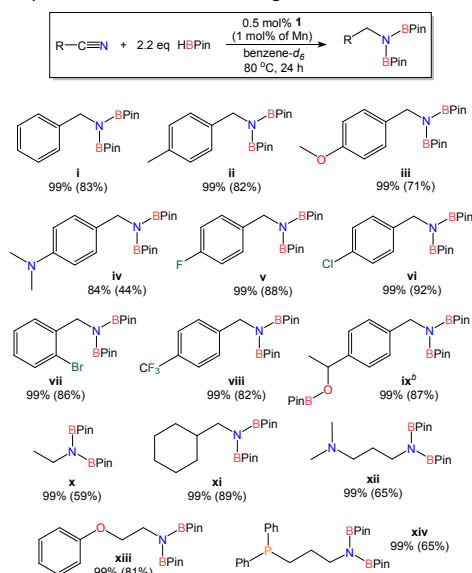
<sup>a</sup>Percent conversion determined by <sup>1</sup>H NMR spectroscopy (integration of residual benzonitrile vs. diborylamine product).

Under the same conditions, 13 additional substrates were screened for **1**-catalysed nitrile dihydroboration (Table 2). Greater than 99% conversion was observed in most cases and modest isolated yields of the respective diborylamines were obtained following recrystallisation. In particular, benzonitrile substitution did not hinder the rate of catalysis and substrates possessing electron-donating (entries ii-iv) and electron-withdrawing (entries v-viii) substituents were reduced. In the case of *p*-acetylbenzonitrile (**ix**), the addition of 3.3 equiv. of HBPin allowed for simultaneous reduction of both the carbonyl and nitrile functionalities. The fact that **1** exhibits activity for carbonyl hydroboration is not surprising, considering that this catalyst was found to hydrosilylate the ketone functionality of 5-hexen-2-one in the presence of PhSiH<sub>3</sub> at ambient temperature.<sup>27</sup> Aliphatic nitriles including acetonitrile (**x**), cyclohexyl nitrile (**xi**), and 2-phenoxyacetonitrile (**xiii**) were successfully converted, as were 3-(dimethylamino)propionitrile (**xii**), and 3-(diphenylphosphino)-propionitrile (**xiv**). These trials indicate that donor substituents do not inhibit the catalytic activity of **1**; an issue

of concern during our efforts to prepare well-defined Co nitrile hydroboration catalysts.<sup>5,22</sup>

To determine the maximum TOF of nitrile dihydroboration, 0.1 mol% of **1** was added to a neat mixture of benzonitrile and HBPin and heated to 80 °C. After 2 h, 52% conversion was observed. However, 6% conversion to diborylamine was detected in the absence of catalyst, rendering the maximum TOF attributable to **1** at 80 °C equal to 230 h<sup>-1</sup> (115 h<sup>-1</sup> relative to Mn).

**Table 2.** Dihydroboration of nitriles using 0.5 mol% **1**.<sup>a</sup>



<sup>a</sup>Percent conversion determined by <sup>1</sup>H NMR spectroscopy (integration of residual benzonitrile vs. diborylamine product) with isolated yield in parentheses. <sup>b</sup>Trial conducted with 3.3 equiv. of HBPin.

**Mechanism.** To determine the mechanism, additional experiments were conducted to identify intermediates relevant to catalysis. First, 2 equiv. of HBPin were added to a solution of **1** in benzene-*d*<sub>6</sub>, but no reaction was observed. In contrast, adding 2 equiv. of benzonitrile to **1** in benzene-*d*<sub>6</sub> resulted in the formation of a yellowish orange product identified as [(2,6-*i*Pr<sub>2</sub>PhBDI)Mn(μ-NCHPh)]<sub>2</sub> (**2**). This compound was found to be paramagnetic (μ<sub>eff</sub> = 6.54 μ<sub>B</sub>, 25 °C) and it exhibits broadened <sup>1</sup>H NMR resonances over a range of 60 ppm.

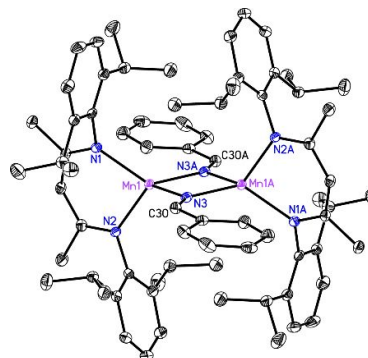


**Figure 2.** The solid-state structure of **2**. Hydrogen atoms have been omitted for clarity.

Single crystals of **2** suitable for X-ray diffraction were obtained upon cooling a concentrated toluene solution layered with pentane to -35 °C (Figure 2). The solid state structure of **2** revealed a short N3-C30 bond length of 1.267(3) Å, indicating that a C=N double bond

remains following nitrile insertion. It should also be pointed out that the Mn–Mn bond length of 3.0819(6) Å in **2** is significantly longer than the 2.8138(7) Å length found for **1**. The full list of metrical parameters for **2** can be found in Table S1 of the ESI.

To obtain additional electronic information, an X-band (9.43 GHz) electron paramagnetic resonance (EPR) spectrum of **2** was collected in a toluene glass at 114 K. The EPR spectrum was found to exhibit a broad and anisotropic signal over 700 mT (Figure 3). As expected, the observed spectral features correspond to a complex in which the two Mn(II) centres are strongly antiferromagnetically coupled (*i.e.*  $|J_0| \gg g\mu_B B_0/h$ ).<sup>27</sup> The EPR spectrum was simulated using a spin Hamiltonian that included the Zeeman and zero-field splitting (ZFS) interactions of the individual Mn(II) ( $S_i = 5/2$ ) sites within the dimer and the dipole-dipole interaction between the two Mn(II) centres.

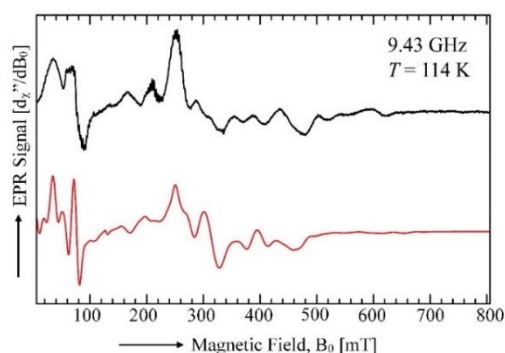


**Figure 3.** The X-band EPR spectrum of **2** at 114 K. The black line is the experimental spectrum and the red line is the simulated spectrum, which was calculated considering the EPR transitions corresponding to the  $S = 1$ ,  $S = 2$ ,  $S = 3$ ,  $S = 4$ , and  $S = 5$  spin states of **2**.

**Table 3.** Parameters used to fit the EPR spectra of **1**<sup>27</sup> and **2** in toluene glass at X-band and low temperature.

Parameter <sup>a</sup>	<b>1</b> <sup>b</sup> ( $T = 106$ K)	<b>2</b> ( $T = 114$ K)
$g_{\text{iso}}$	2.05	2.06
$D$	0.0932	0.1153
$ E/D $	0.138	0.256
$J_x$ ( $\text{cm}^{-1}$ )	-0.0089	-0.0061
$J_y$ ( $\text{cm}^{-1}$ )	-0.0036	-0.0015
$J_z$ ( $\text{cm}^{-1}$ )	0.0125	0.0076
$\Delta B$ (MHz)	600	600

<sup>a</sup>The fitting parameters were the isotropic  $g$ -value,  $g_{\text{iso}}$ , the zero-field splitting parameters,  $D$  and  $E$ , the principal components of the dipole-dipole interaction tensor  $J$ , (*i.e.*  $J_x$ ,  $J_y$ , and  $J_z$ ), and the isotropic line width,  $\Delta B$ . <sup>b</sup>Data from reference 27.

The best fit was obtained considering the EPR transitions corresponding to the total spin manifolds  $S = 1, 2, 3, 4$ , and  $5$ . The parameters obtained from the fit are shown in Table 3 and correspond to high-spin Mn(II) centres.<sup>27</sup> However, the rhombic distortion of the ZFS interaction (*i.e.*  $|E/D|$ ) obtained for **2** (0.256) is significantly larger than the one previously reported for **1** (0.138). This result suggests that the larger bridging ligand in **2** (*i.e.* NCHC<sub>6</sub>H<sub>5</sub>) introduces larger electrostatic distortions to the crystal field surrounding the Mn(II) ions. Furthermore, the value of  $J_z$  obtained for **2** (0.0076  $\text{cm}^{-1}$ ) is considerably smaller than that obtained earlier for **1** (0.0125  $\text{cm}^{-1}$ ).  $J_z$  is the principal component of the dipole-dipole interaction tensor along the Mn(II)–Mn(II) axis and its value is to first order proportional to the inverse of the Mn(II)–Mn(II) distance to the

third. Thus, the smaller value of  $J_z$  observed for **2** indicates a longer Mn(II)–Mn(II) distance, which agrees with the crystallographically determined Mn–Mn bond lengths in **2** (3.08 Å) and **1** (2.81 Å).

Importantly, **2** was found to mediate the dihydroboration of benzonitrile under the same conditions as **1**, suggesting that it is an intermediate relevant to catalysis. To clarify this hypothesis and construct a complete catalytic cycle, density functional calculations (DFT) were performed. Figure 4 summarises the most likely mechanism for dihydroboration. We assigned an open-shell singlet state for the ground state of **1**, where five unpaired electrons of one Mn centre are antiferromagnetically coupled to the electrons of the other Mn centre. Given that spin crossover is easy for first-row metals, all plausible spin states were taken into account, and we found a sextet ground state for all of the monomeric species, exhibiting good agreement with the observed solution magnetic susceptibility data of 6.0  $\mu_B$  (25 °C) for the related monomeric intermediate, (<sup>2,6-*i*Pr<sub>2</sub>Ph</sup>BDI)Mn(CH(CH<sub>3</sub>)(4-*t*BuPh)).<sup>27</sup>

The energy difference between **1** and the corresponding monomer (**6A**) is calculated to be 1.5  $\text{kcal mol}^{-1}$ , indicating that the monomeric species is readily available in solution. In our calculations, we employed benzonitrile as a representative substrate and found that it can bind to the active catalyst **6A** to furnish intermediate **6B** at 5.1  $\text{kcal mol}^{-1}$ . The nitrile group is inserted into the Mn–H moiety through **6B-TS** with a barrier of 17.1  $\text{kcal mol}^{-1}$ . Having an overall barrier of 22.2  $\text{kcal mol}^{-1}$  during the first reduction cycle, the insertion step is exergonic and is mediated by the formation of a stable C–H bond in imino(amide) complex **6C**. In accordance with the fact that **2** is isolable, dimerisation of **6C** to afford **2** features a relative energy of -22.5  $\text{kcal mol}^{-1}$ . While the formation of **2** might be preferred due to electron-deficient nature of **6C**, dissociation of **2** is accessible to regenerate catalytically relevant **6C** at the given reaction temperature of 80 °C.

Competing with the dimerisation, consumption of HBPIn drives the reaction to proceed further. Binding of HBPIn to **6C** leads to a stable Lewis acid-base pair **6D** which temporarily adopts an *O*-bound conformation. The following endothermic rearrangement gives **6E** at -4.2  $\text{kcal mol}^{-1}$ . Its characteristic Mn–H–B–N metallacycle pre-activates the B–H bond, allowing  $\sigma$ -bond metathesis to occur traversing a pseudo-transition state, **6E-TS**. Although the resulting Mn–H complex **6F** may formally release the borylimine to access **1K**, our computation suggests that the dissociation is reversible to regenerate **6F**, which will undergo insertion to generate the stable Mn-amido complex **1G** located at -31.4  $\text{kcal mol}^{-1}$ . The overall barrier starting from **2** to the second insertion transition state, **6F-TS**, is 32.0  $\text{kcal mol}^{-1}$ . It is affordable at 80 °C and consistent with the prolonged reaction time (24 h). Association of second equivalent of HBPIn generates intermediate **6H** involving the aforementioned metallacycle. In this case, the *H*-bound conformation is favoured over the *O*-bound conformation (Fig. S36) due to steric congestion between the BPin moiety and bulky substituents on the BDI framework. Finally,  $\sigma$ -bond metathesis regenerates the active catalyst **6A** to furnish the final product, *N,N*-diborylamine. Based on the mechanism, we suspect that the Lewis acidity of 9-BBN renders it inactive for nitrile dihydroboration due to formation of a stable Lewis acid/base pair<sup>28</sup> with **6C**, which raises the barrier for  $\sigma$ -bond metathesis to the point where it cannot be accessed at 80 °C.

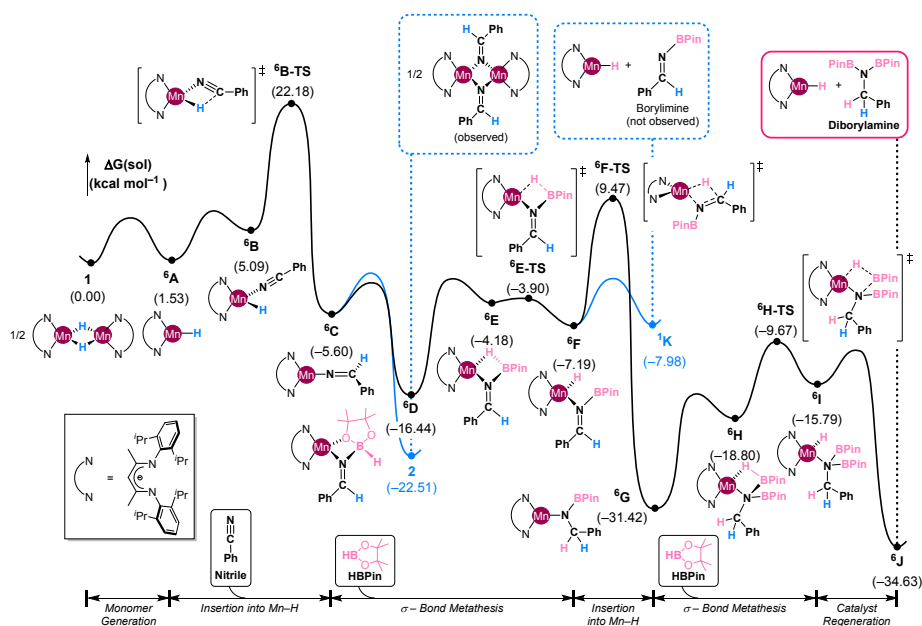


**Figure 4.** DFT-calculated energy profile of **1**-catalysed benzonitrile dihydroboration.

In summary, the dihydroboration of nitriles to yield *N,N*-diborylamines has been demonstrated for the first time using a well-defined manganese catalyst. Broad functional group tolerance was observed at relatively low catalyst loadings. Experimental and computational studies reveal that **1**-catalysed nitrile dihydroboration proceeds following insertion into the Mn–H moiety, followed by  $\sigma$ -bond metathesis between amide monomers and incoming HBPin.

**Acknowledgements.** This material is based upon work supported by the National Science Foundation under Grant No. 1651686. MHB acknowledges the financial support from Institute for Basic Science (IBS-R10-A1).

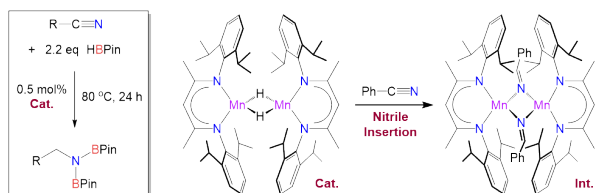
## Conflicts of interest

T.T.N. and R.J.T. retain rights to catalysts **1** and **2** through U.S. Patent Application Nos. 62/678,624 and 16/407,317.

## Notes and references

- M. Suginome, L. Uehlin and M. Murakami, *J. Am. Chem. Soc.*, 2004, **126**, 13196–13197.
- A. Y. Khalimon, P. M. Farha and G. I. Nikonov, *Dalton Trans.*, 2015, **44**, 18945–18956.
- T. Kitano, T. Komuro and H. Tobita, *Organometallics*, 2019, **38**, 1417–1420.
- G. P. Junor, E. A. Romero, X. Chen, R. Jazzar and G. Bertrand, *Angew. Chem. Int. Ed.*, 2019, **58**, 2875–2878.
- C. Ghosh, S. Kim, M. R. Mena, J.-H. Kim, R. Pal, C. L. Rock, T. L. Groy, M.-H. Baik and R. J. Trovitch, *J. Am. Chem. Soc.*, 2019, **141**, 15327–15337.
- A. Y. Khalimon, P. Farha, L. G. Kuzmina and G. I. Nikonov, *Chem. Commun.*, 2012, **48**, 455–457.
- J. B. Geri and N. K. Szymczak, *J. Am. Chem. Soc.*, 2015, **137**, 12808–12814.
- A. Kaithal, B. Chatterjee and C. Gunanathan, *J. Org. Chem.*, 2016, **81**, 11153–11161.
- C. Weetman, M. D. Anker, M. Arrowsmith, M. S. Hill, G. Kociok-Köhn, D. J. Liptrot and M. F. Mahon, *Chem. Sci.*, 2016, **7**, 628–641.
- J. Li, M. Luo, X. Sheng, H. Hua, W. Yao, S. A. Pullarkat, L. Xu and M. Ma, *Org. Chem. Front.*, 2018, **5**, 3538–3547.
- G. Nakamura, Y. Nakajima, K. Matsumoto, V. Srinivas and S. Shimada, *Catal. Sci. Technol.*, 2017, **7**, 3196–3199.
- M. Ito, M. Itazaki and H. Nakazawa, *Inorg. Chem.*, 2017, **56**, 13709–13714.
- A. D. Ibrahim, S. W. Entsminger and A. R. Fout, *ACS Catal.*, 2017, **7**, 3730–3734.
- Z. Huang, S. Wang, X. Zhu, Q. Yuan, Y. Wei, S. Zhou and X. Mu, *Inorg. Chem.*, 2018, **57**, 15069–15078.
- A. Harinath, J. Bhattacharjee and T. K. Panda, *Adv. Synth. Catal.*, 2019, **361**, 850–857.
- W. Liu, Y. Ding, D. Jin, Q. Shen, B. Yan, X. Ma and Z. Yang, *Green Chem.*, 2019, **21**, 3812–3815.
- Y. Ding, X. Ma, Y. Liu, W. Liu, Z. Yang and H. W. Roesky, *Organometallics*, 2019, **38**, 3092–3097.
- S. Saha and M. S. Eisen, *ACS Catal.*, 2019, **9**, 5947–5956.
- I. Banerjee, S. Anga, K. Bano and T. K. Panda, *J. Organomet. Chem.*, 2019, **902**, 120958.
- S. Das, J. Bhattacharjee and T. K. Panda, *New J. Chem.*, 2019, **43**, 16812–16818.
- X. Feng, P. Ji, Z. Li, T. Drake, P. Oliveres, E. Y. Chen, Y. Song, C. Wang and W. Lin, *ACS Catal.*, 2019, **9**, 3327–3337.
- H. Ben-Daat, C. L. Rock, M. Flores, T. L. Groy, A. C. Bowman and R. J. Trovitch, *Chem. Commun.*, 2017, **53**, 7333–7336.
- R. J. Trovitch, *Synlett*, 2014, **25**, 1638–1642.
- M. Garbe, K. Junge and M. Beller, *Eur. J. Org. Chem.*, 2017, **2017**, 4344–4362.
- R. J. Trovitch, *Acc. Chem. Res.*, 2017, **50**, 2842–2852.
- X. Yang and C. Wang, *Chem. Asian J.*, 2018, **13**, 2307–2315.
- T. K. Mukhopadhyay, M. Flores, T. L. Groy and R. J. Trovitch, *Chem. Sci.*, 2018, **9**, 7673–7680.
- H. Song, K. Ye, P. Geng, X. Han, R. Liao, C.-H. Tung and W. Wang, *ACS Catal.*, 2017, **7**, 7709–7717.

## TOC Graphic:



Nitrile insertion allows for manganese-catalyzed nitrile dihydroboration at  $80\text{ }^\circ\text{C}$ .